NASA
Technical
Paper
2400

c.2

March 1985

Parametric Study of a Canard-Configured Transport Using Conceptual Design Optimization

P. Douglas Arbuckle
and Steven M. Sliwa

NASA

NASA
Technical
Paper
2400

1985

Parametric Study of a Canard-Configured Transport Using Conceptual Design Optimization

P. Douglas Arbuckle
and Steven M. Sliwa

Langley Research Center
Hampton, Virginia

NASA

National Aeronautics
and Space Administration

Scientific and Technical
Information Branch

Summary

Constrained-parameter optimization is used to perform optimal conceptual design of both canard and conventional configurations of a medium-range transport. A number of design constants and design constraints are systematically varied to compare the sensitivities of canard and conventional configurations to a variety of technology assumptions. Main-landing-gear location and canard surface high-lift performance are identified as critical design parameters for a statically stable, subsonic, canard-configured transport.

Introduction

As new technologies or major configuration changes are proposed for incorporation into aircraft design, a debate is usually waged on the relative merits of changing current design practice. Often this debate is not held when obvious technological advances are being proposed. However, proposals are periodically made which cause exhaustive debate within the technical community. Such is the case with the current debate concerning the relative merits of canard configurations versus conventional aft-tail configurations. Historically, early canard designs suffered pitch divergence problems (i.e., they were unstable); the sometimes fatal consequences of flying these aircraft caused most designers to avoid canard configurations (ref. 1). The recent success of canard-configured ultralight and homebuilt aircraft has revived the canard argument. Both sides in this debate have sought to prove the general superiority of either a canard configuration or a conventional aft-tail configuration. The intuitive appeal of using a lifting surface for trim is undeniable, but analyses and comparisons of canard and conventional configurations are far more complex. The current consensus is that canard and conventional configurations can only be fairly compared with one another for a given mission or missions. For example, a conventional medium-range transport can hardly be compared with a canard-equipped two-seat sport aircraft such as the Rutan VariEze.

To compare canard and conventional configurations, a systematic methodology must be developed. At the Langley Research Center, a preliminary transport aircraft design tool has been developed to reliably assess the potential payoffs of various new technologies (ref. 2). This tool is the computer program OPDOT (Optimum Preliminary Design of Transports). The OPDOT program has been successfully used to perform studies evaluating the following: (1) the sensitivity of a transport design to relaxed static-stability augmentation systems; (2) the impact of choosing unaugmented longitudinal flying-qualities design criteria; and (3) the sensitivity of a transport design to a variety of economic and technological assumptions (refs. 3 to 6). The basic OPDOT code has been enhanced and modified so the program can be used to analyze both canard and conventional transport configurations.

This "new" OPDOT program has been used to conduct a study identifying some of the critical design parameters of a statically stable medium-range canard-configured transport and a similarly configured tandem-wing transport. A conventional, statically stable medium-range transport was also studied in parallel to provide a performance benchmark with which canard configurations and tandem-wing configurations could be compared. Each configuration was evaluated and optimized on the basis of an economic performance index of interest to the airlines. This performance index—the income required per flight for a fixed return on investment—is a straightforward measure of the cost of operating a transport aircraft. The results of the study, in which a canard configuration was compared with a conventional configuration, are presented in this paper.

Symbols

AR	aspect ratio
$B*$	maximum Brequet range factor
$C_{A\$}$	aircraft purchase price, U.S. dollars
C_L	lift coefficient
C_{L_α}	lift-curve slope, per radian
C_m	pitching-moment coefficient
$C_{m,o}$	wing-body zero-lift pitching-moment coefficient
c.g.	center of gravity
DOC	direct operating cost, U.S. dollars per hour
FARE	income required per flight for a fixed ROI, U.S. dollars
h_{cr}	cruise altitude, ft
IOC	indirect operating cost, U.S. dollars per hour
k	factor for converting hourly income to income per flight
L	lift, normalized by dynamic pressure, ft^2

L/D	lift-drag ratio
l_f	fuselage length, ft
M_{cr}	cruise Mach number
M_o	wing-body zero-lift pitching moment, normalized by dynamic pressure, ft^3
MAC	mean aerodynamic chord
NG	nosewheel steering traction margin, percent MAC
ROI	annual return on investment, percent
S	surface area, ft^2
SM	minimum static margin, $100(x_{np} - x'_{cg})$, percent
T	installed thrust, lb
t_r	annual tax rate
U	annual utilization, hour
V_p	passenger volume, ft^3
W	aircraft weight, lb
$\bar{x}$	longitudinal distance from aircraft c.g., ft
x_{cg}	longitudinal position of c.g., percent MAC
x'_{cg}	longitudinal position of aftmost c.g., percent MAC
x_{lg}	main-landing-gear longitudinal position, percent MAC
x_{np}	longitudinal position of stick-fixed neutral point, percent MAC, where $dC_m/dC_L = 0$
x_{st}	horizontal-stabilizer longitudinal position, percent l_f
z	vertical distance from aircraft c.g., ft
α	angle of attack, deg
μ	coefficient of rolling friction

Subscripts:

av	available
max	maximum
lg	landing gear
req	required
st	stabilizer, horizontal trimming surface
Tl	thrust line
w	wing

Survey of Canard Research

Over the years, a variety of research has been conducted on canard configurations. Reference 1 gives a fairly comprehensive historical overview of the published research to date. Many classes of aircraft have been the subjects of canard research, including fighters, supersonic bombers, and general aviation aircraft. After initial use by the Wright brothers, the canard arrangement has not been widely considered or used until recently.

References 7 and 8 are representative of the wind tunnel research conducted on canard configurations. Reference 7 describes a study of various planforms at supersonic speeds. The planforms examined are typical of fighters or supersonic bombers. This paper, one of many written about supersonic canard configurations during that time period, concludes that the trim drag characteristics of a canard configuration are superior to a conventional configuration and that any interference effects created by the canard are minor or can be alleviated with proper design. Reference 8 is a compilation of wind tunnel data supplementing previous NASA reports which conclude that close-coupled canard configurations provide substantial improvements in fighter maneuverability.

References 9 to 13 describe typical theoretical research examining canard configurations. Reference 9 compares canard and conventional configurations by using minimum drag with trim and static-stability constraints and concludes that conventional configurations have generally lower drag than canard configurations. Further, it notes that most canard configurations (except for those with near-zero span ratios) are more sensitive (in induced drag) to static-margin variations.

References 10 and 11 are similar in scope and content. The research described in these reports compares canard and conventional configurations by using drag with static-stability constraints and including weight effects. Reference 10 concludes that the superiority of conventional configurations has a sound theoretical basis, although conventional configuration performance could be improved. Also, this paper notes that analysis techniques which account for “roll up” of the canard-surface flow onto the wing are not required for typical “long-coupled” canard configurations (those with a streamwise gap of about 400 percent MAC), since the vortex position on the wing does not affect interference drag by more than a few percent.

Reference 12 builds on the work of references 9 and 14 and concludes that a close-coupled three-surface configuration (configuration with both a canard and an aft tail) is superior to either close-coupled canard or conventional configurations. This paper also notes the theoretical basis for modifying the classic Prandtl-Munk theory to properly account for the effect of the canard-surface downwash on the wing. This modification results in an induced-drag reduction of approximately 5 to 10 percent from that predicted with the classic theory. This induced-drag reduction is also indicated from wind tunnel testing (ref. 15).

Reference 13 describes theoretical research of two interacting lifting surfaces. The effects on minimum induced drag are examined for various lift distributions and span ratios. The effect of gap ratio is also examined. No consideration is given to static stability or to other constraints. This paper concludes that canard configurations require a nonzero gap ratio sufficiently large so the canard surface can "carry its share" at the minimum-drag condition.

References 16 to 22 describe wind tunnel and theoretical or design studies of canards applied to general aviation or commuter-class aircraft. Reference 16 examines a modified version of a popular homebuilt kit aircraft described in reference 17. The impact on performance of loss of laminar flow is noted, as is the effectiveness of the canard surface in limiting angle of attack and increasing stall-departure resistance. Reference 18 describes the stall characteristics and vehicle stability for various angles of attack of a canard-configured general aviation prototype. The sensitivity of the configuration to c.g. movement and power effects is significant.

References 19 to 21 describe aerodynamic evaluations of canard and conventional general aviation configurations. Reference 19 is a study of the generic effects on drag of stagger and decalage (difference between the angles of incidence of the wing and the canard) of a close-coupled canard configuration. Reference 20 examines a 6-passenger and a 12-passenger general aviation configuration with either a conventional aft tail or a canard, and it concludes that general aviation configurations with "stall-proof" canards cannot outperform conventional configurations. In this study, minimum drag is measured as various geometric parameters are changed. The values for aspect ratio and stagger are comparable to jet transport values, but wing loading is limited to 60 lb/ft^2 and the gap ratios used may not be achievable by transport designs. Reference 21 is a parametric study of a general aviation canard configuration and concludes that although conventional configurations have a lower minimum drag, canard configurations are less sensitive to off-optimum conditions.

Reference 22 is a preliminary design investigation of a 30-passenger commuter configuration with either a conventional aft tail, a canard surface, or both (a three-surface configuration). This paper concludes that a three-surface configuration is superior to either a canard or a conventional configuration. The paper also notes that it is impractical to design a high-wing-loading canard configuration with inherent static stability.

The research described in the present paper, which compares conventional aft-tail configurations with canard configurations, is unique because of the following:

1. This research is the first comprehensive design study of subsonic, medium-range transport aircraft with canards.
2. The choice of a commercial-transport-class aircraft enables, for the first time, the use of economic performance measures as the design figure of merit during trade studies.
3. The research includes all effects normally required at the preliminary design stage, such as induced drag, parasite drag, trim drag, weight, stability, and near-optimal mission profiles. Only references 20 and 22 include nearly this level of detail.
4. A systematic optimization scheme is used to find the "best" canard configuration for the given mission and technology constraints.
5. This is the first reported research in which conventional aft-tail and canard configurations are designed for the same mission with the same constraints. Fair comparisons are then possible for the class of aircraft considered.

This research indicates that there are two critical design problems for canard configurations. One is well understood and recognized in the literature but severely limits the performance of this class of aircraft. The other design problem is unique to this class of aircraft. Both problems are detailed in this paper.

Method of Calculation

General

The general optimization scheme for OPDOT is shown in figure 1. Nominal values for a set of independent design variables are used as input along with the required design constants for specifying fixed geometries, mission economic factors, mission profile data, and the nonlinear aerodynamic terms. The nine independent design variables chosen for this study are shown in table I along with the allowable ranges, which act as directly applied side constraints. Wing area and wing aspect ratio are selected as design variables since they have the most impact upon the aircraft sizing. Horizontal-stabilizer sizing is accomplished by including horizontal-stabilizer area, horizontal-stabilizer aspect ratio, horizontal-stabilizer longitudinal position, center-of-gravity position, and main-landing-gear longitudinal position as independent design variables. Finally, fuselage length and installed thrust are used as independent design variables to match the aircraft size to the mission and to the wing planform.

The set of independent design variables is incremented by the optimizer logic in an attempt to improve the design. The value of the performance index (parameter to be optimized) is determined from the values of the independent design variables and from information in the communications module. This index is selected from a list of possible performance indices. The performance index used for these studies is the income required per flight for a fixed return on investment (FARE). The merits of using this index are described in references 3 and 4.

The constraint functions (involving inequality relationships) represent operational, flying-qualities, and performance constraints and are based upon certification regulations, mission definition, and practical considerations. It should be noted that no flying-qualities constraints are considered in this study. Constraints are integrated into the optimization process by adding a penalty to the performance index for each constraint violation. Each penalty term is proportional to the square of the violation times a weighting factor. The performance index plus these penalty terms form an augmented performance function. If the weighting factor is sufficiently large, minimizing the augmented performance function is equivalent to finding the minimum performance index while satisfying all the constraints.

Optimization Technique

The numerical optimization logic, which iterates the independent design variables to minimize the augmented performance function, is a subject of intense research in nearly all fields of engineering. Previous studies and the authors' experience indicate that various gradient methods suffer from numerical difficulties when analytical equations are not available to provide the gradients and also from initialization problems when the number of active constraints is large with respect to the number of independent design variables. When aircraft design is posed as a numerical optimization problem, the analytical gradients generally will not be available and an initially feasible solution to start the optimization scheme may be difficult to locate. A direct, sequential-search simplex algorithm is used to overcome these difficulties (refs. 3, 23, and 24). During the iteration, the optimizer routine which contains the sequential simplex algorithm sends the values of the independent design variables and the design constants to the performance-index evaluation routines. A schematic representation of the calling sequence for the performance-index evaluation routines is shown in figure 2.

Evaluation of Unaugmented Performance Index

Aircraft weight is estimated by iteration. Most component weight relations, including fuel weight, are functions of gross weight as well as geometry. The design mission is simulated and repeated until the hypothesized gross take-off weight at the beginning of a weight iteration approaches the sum of the individual aircraft component weights, the payload, and the fuel weight. The convergence criterion for the weight iteration is chosen to ensure numerical accuracy, which is important for optimizer performance. However, the relations used to compute weights are from industry statistics and are only expected to be accurate to within 10 percent. Industry statistics for the aircraft component weights come from references 25 to 28 and are functions of all the independent design variables, the gross take-off weight, and approximately 20 of the design constants input through the communications module. For canard configurations, the statistical weight relations are modified such that the wing weight and the horizontal-stabilizer weight reflect the division of lift load between these two surfaces. The fuel weight is calculated by summing estimates of the required fuel for the following mission segments: taxi, take-off and climb, cruise, descent, and reserve.

The mission profile as modeled is shown in figure 3. It consists primarily of a multiple-step cruise-climb approximation of an optimal fuel profile. The cruise portion is broken into 10 equally spaced segments, and Breguet-type relationships are used for calculating the amount of fuel burned during each segment (ref. 25). Comparisons of this discrete flight path with continuously optimal flight profiles (ref. 29) show differences of less than 5 percent. Thus, the Breguet-type relationships are good approximations for comparative design studies. Engine performance is computed based on the TF39-GE-1 engine used on the C-5A aircraft (ref. 29). The baseline engine is "rubberized" as required with standard scaling laws to achieve the required installed thrust for the prescribed mission.

Parasite drag for all flight phases is calculated from a component buildup including compressibility and Reynolds number effects using the methods of references 25 and 28 to 31. Induced drag for all phases of flight is estimated by using nonlinear corrections to parabolic drag polars for airfoil-section camber (ref. 32) and by adding terms for the tail induced drag and wing-tail interference drag (ref. 9). Wind tunnel results and theoretical analysis (refs. 10, 12, and 15) indicate the total induced drag for canard configurations similar to the type considered here will be up to 10 percent less than that indicated by conventional theoretical methods. Therefore, the total induced drag for canard configurations is empirically reduced 10 percent from that estimated with the above methods (refs. 9 and 32). Calculations of stability and control derivatives for all flight phases are typical of those used in preliminary design (refs. 33 and 34) and include empirical adjustments from aerodynamic wind tunnel and flight data (refs. 35 to 39) for compressibility, elasticity, and the use of supercritical airfoil sections. Ground-effect calculations used in the take-off control-power calculations are from reference 33. A trim routine is used for determining the wing and tail loads in cruise, take-off, and approach phases of flight. This trim routine is simplified from the routine used in reference 2 by assuming that the resultant drag vector acts through the aircraft c.g., yielding no contribution to aircraft pitching moment. This assumption permits the "drag terms" in the longitudinal trim equation to be ignored; the resulting trim equation is referred to as the "simple trim equation" in subsequent discussions. Throughout the flight envelope, the simple trim routine yields results within 10 percent of the results from a more exact, computationally intensive routine described in reference 2.

The cost data are approximated from industry statistics for manufacturing, maintenance, and other components of direct operating costs as well as the indirect operating costs (refs. 25, 27, and 40 to 43). The direct operating cost is an augmented form of the industry standard (ref. 3). FARE is calculated in the following manner:

$$\text{FARE} = \left[\frac{0.9C_{A\$}(\text{ROI})(0.01)}{(1-t_r)U} + \text{DOC} + \text{IOC}\right] k$$

Desired return on investment (ROI) in percent, multiplied by the aircraft purchase price $C_{A\$}$ minus the 10 percent investment tax credit is the annual return on investment in dollars per year. Dividing this term by the quantity 1 minus the tax rate t_r times the annual utilization U yields the pretax hourly ROI, or profit. Adding direct operating cost (DOC) and indirect operating cost (IOC) gives the income required per hour, and multiplying by k, a factor for converting hourly income to income per flight, converts this result to income required per flight (FARE).

The absolute accuracy of the performance index (in this case FARE) is only expected to be approximately 10 percent. In reality, the accuracy may be even less, since any systematic computation of an aircraft purchase price based on the costs incurred by the manufacturer is impossible. However, with the level of detail included in OPDOT, the relative accuracy is quite good for comparing "similar" configurations. This observation has been borne out by previous studies (refs. 3 to 6) and by comparing results from OPDOT with an independent study (ref. 44).

OPDOT Baselines

To provide a basis for performing the trade studies, a baseline mission is chosen. Table II lists the design constants chosen for the baseline mission that are used along with the independent design variables and constraint functions listed in table I. Note that each of the baseline configurations (see table III)—conventional, canard, and tandem wing—have at least a 10-percent-stable static margin.

Several design constants have different values for the canard and conventional baseline configurations. (See table II.) Specifically, these design constants are the wing and horizontal-stabilizer sweep angles, the horizontal-stabilizer height above centerline, and the wing longitudinal position along the fuselage. Originally, both sweep angles and the wing position were treated as independent design variables. However, initial studies showed that these three design parameters were insensitive to constraint and mission changes (typically the values for these parameters varied by less than 5 percent). Therefore, the wing and horizontal-stabilizer sweep angles and the wing longitudinal position are made design constants at their nominal values, which differ for the canard and conventional configurations. The horizontal-stabilizer height is chosen from geometric considerations. For the conventional configuration, the horizontal-stabilizer root is placed about 2 ft below the vertical-stabilizer–fuselage juncture. For the canard configuration, the horizontal stabilizer is placed such that it is above the wing yet below the passenger-cabin floor. Although this position is not aerodynamically optimal, it is expected to have little adverse impact for the long-coupled (longitudinal separation distances in excess of 300 percent MAC) canard configuration considered (ref. 15).

The sensitivity of a transport design to variations in mission definition and design constraints is determined for these studies by using OPDOT in the manner shown in figure 4. Design variables, design constants, and design constraints are input to OPDOT, which generates an optimal conceptual design. Then, a design constant or design constraint of interest is changed and OPDOT generates a new resized design, optimized to minimize FARE. This process is repeated until a set of designs have been generated for a given design parameter. The sensitivity of the design to the varied design parameter is determined by examining the variation of optimum, or converged, FARE values as the design parameter is changed.

For the purpose of comparison, baseline conceptual designs are developed for the conventional, canard, and tandem-wing configurations. Table III shows the values of the design variables for these baseline conceptual designs. Figures 5 to 7 show, respectively, graphics output from OPDOT of the baseline conventional configuration, the baseline canard configuration, and the baseline tandem-wing configuration. The tandem-wing configuration is similar to the canard configuration. However, for a tandem-wing configuration the two lifting surfaces are geometrically identical. This means that for each lifting surface, the aspect ratio, the taper ratio, the thickness ratio, and the area are equivalent. It has been argued that economic savings will result from this design because of reduced tooling requirements and production-learning-curve considerations, but these savings have not been considered in this study. For the conventional configuration, two baselines were initially developed. One baseline conventional configuration was sized with x_{lg} (the main-landing-gear position) as a design variable free to move longitudinally along the fuselage to a location determined to be optimum by OPDOT as long as it remained 20 percent MAC behind x'_{cg}. The other conventional baseline was sized with x_{lg} held constant at 65 percent MAC. This is the position selected during the initial Integrated Application of Active Controls (IAAC) studies (ref. 44). The differences between these two baseline conventional configurations were very small over a wide range of design conditions; therefore, only the conventional configuration with constant x_{lg} is considered in this paper.

Initial OPDOT runs indicated that the program would not converge to a constrained solution for a canard configuration. It was observed that the approach C_L for canard configurations was abnormally low. Analysis of a generic canard configuration was performed in order to gain insight into the problem. Appendix A indicates that by considering a simple trim equation and a simple static-stability equation, it is possible to show that the allowable $C_{L,\max}$ on the horizontal stabilizer of a canard configuration must exceed that of the wing. The canard-surface $C_{L,\max}$ constraint in OPDOT originally had the same value as for a conventional configuration. In view of the results from appendix A, the allowable $C_{L,\max}$ of the canard surface is increased to the value allowed for wing $C_{L,\max}$, which is close to the maximum achievable C_L for a given lifting surface with a triple-slotted flap.

Results and Discussion

A study of the effect of varying landing and take-off field lengths is conducted to compare conventional and canard configurations, since landing and take-off field length is one of the most critical mission constraints with respect to configuration sizing (refs. 3 and 32). The sensitivity of all configurations to changes in take-off and landing field-length constraints is shown in figure 8. As expected, designing for shorter field lengths increases FARE, decreasing the economic efficiency of the design. The sensitivity of the tandem-wing configuration to variations in field length approximates the sensitivity of the canard configuration for all field lengths. This is expected because a tandem-wing configuration is essentially a special type of a canard configuration. Note that the tandem-wing configuration requires about 2 percent more FARE (about $800 per flight) than the canard configuration. This would seem to indicate that a tandem-wing configuration is a less efficient design than a canard configuration, unless the postulated production savings are large enough to offset this lower efficiency. The canard configuration suffers incrementally less in FARE penalties than does the conventional configuration for the shorter field lengths. A canard configuration requires at least 2 percent less FARE than a conventional transport design for all field lengths. This result can be misleading because of several unrealistic (but necessary) assumptions that are made inherently within OPDOT to obtain satisfactory convergence for canard designs.

The first of these inherent assumptions is that the canard-surface $C_{L,\max}$ is permitted to exceed a value of 0.8 without any cost, weight, or drag penalties. Recall that the weight and drag equations are only modified to account for the lift load carried by the canard surface. Addition of a flap system to the canard surface, necessary for $C_{L,\max}$ exceeding approximately 1.0, will invoke cost, weight, and drag penalties. Typical industry practice is to constrain the $C_{L,\max}$ of the horizontal stabilizer to less than 0.8 for all trimmed-flight conditions. The impact of varying canard-surface $C_{L,\max}$ is shown in figure 9. Note that the selected value for canard-surface $C_{L,\max}$ of 3.15 for the baseline canard configuration provides approximately the minimum FARE. Achieving this $C_{L,\max}$ requires a triple-slotted flap system on the canard. The data of figure 9 indicate a large penalty in optimum FARE as canard-surface $C_{L,\max}$ is reduced, because the horizontal-stabilizer $C_{L,\max}$ effectively sizes the overall canard-configuration design. Clearly, a complex flap system is required for economically viable canard transport designs.

A second assumption inherent to OPDOT is that the main landing gear can be moved longitudinally away from the wing structure with no weight, cost, or drag penalties. The weight and cost penalties are associated with designing and producing a transport aircraft for which the main gear is dislocated from the wing structure and, therefore, cannot take structural advantage from attaching to it. The drag penalty is associated with adding pods or nacelles to house a landing-gear system not located in the wing (such as for a C-130 transport). The sensitivity of the canard configuration to main-landing-gear position is shown in figure 10. Notice the extreme sensitivity of FARE as the main gear is moved toward the wing. This is due to the sensitivity of the take-off control-power calculation to the distance between the main gear and the aircraft c.g., especially for canard configurations. For a heuristic discussion of take-off control-power requirements, see appendix B. OPDOT cannot find a satisfactory canard configuration with a main-landing-gear position aft of −70 percent MAC. This position is still slightly forward of the wing-root leading edge, so that the main landing gear will be remotely located from the wing structure, as stated above.

With the assumption that future studies might establish the cumulative weight penalties inherent in providing an adequate canard-surface flap system and remotely locating the main landing gear from the wing, an attempt is made to document the impact of additional weight and drag on the canard configuration. Figure 11 shows the increase in FARE as the weight is increased from the baseline configuration. Note that each data point represents a resized design after the weight penalty is added. If the weight penalty exceeds approximately 2500 lb (approximately 1 percent of maximum gross take-off weight), FARE for the canard configuration exceeds FARE for the baseline conventional configuration. Cost penalties due to design and certification of a high-lift canard surface and the main landing gear dislocated from the wing structure will further penalize the canard configuration. The sensitivity of canard and conventional transport designs to drag variations is documented in figure 12. The drag variations are obtained by varying only the wing parasite drag. Variations in drag affect both conventional and canard configurations equally.

Up to this point, all sensitivity studies have been conducted with statically stable configurations. It has been suggested that relaxing minimum-static-margin requirements will benefit a canard configuration more than it will a conventional one (ref. 11). Specifically, if negative static margins are allowed by providing relaxed static-stability augmentation systems, the performance of a canard configuration might be significantly improved. Changes in the minimum static margin are accomplished by changing the static-margin constraint and allowing OPDOT to resize each configuration to take advantage (or, for changes to more stable static margins, minimize the disadvantage) of the new static-stability requirement. The impact of relaxing the static-stability requirement on canard, conventional, and tandem-wing configurations is shown in figure 13. The percent change in FARE is used as the measure of sensitivity to static-margin variations. For minimum static margins less than 5 percent stable, the canard configuration shows less sensitivity to static-margin changes than does the conventional configuration.

Examination of the canard configuration shows that as the minimum static margin is decreased to values less than 5 percent stable, the C_L of the canard surface decreases, which causes the wing C_L to increase to maintain overall C_L. The resulting increase in wing induced drag is greater than the decrease in canard-surface induced drag, causing a slight increase in overall induced drag. This drag increase causes compromises in the design, decreasing the sensitivity of the canard configuration to relaxation of the static-margin constraint; therefore, unstable static margins will not be as beneficial for canard configurations as for conventional configurations.

The tandem-wing configuration shows little sensitivity to changes in minimum static margin down to 2 percent static stability. Forcing the minimum static margin below 2 percent stable has an extremely adverse economic effect on the design. This occurs because it is necessary to move the aircraft c.g. well aft of the baseline position to achieve negative static margins. This c.g. movement, coupled with the need for aircraft trim, requires adjustments of C_L between the two lifting surfaces similar to those that caused compromises in the canard configuration. However, for the tandem-wing configuration with its limited degrees of freedom in the design variables, this C_L adjustment is far more critical.

Variations in canard-surface sweep angle are made to verify the observed insensitivity of the design to this parameter. (See "OPDOT Baselines" section.) The effect of varying canard-surface sweep angle is shown in figure 14. Varying the sweep appears to have little impact on FARE. Reduction in horizontal-stabilizer sweep angle increases stabilizer C_{L_α} and allows a size reduction of the horizontal stabilizer and a potential reduction in FARE. However, the increases in compressibility drag that result as the sweep angle is reduced balance the beneficial effects of increasing stabilizer C_{L_α}.

Concluding Remarks

The research described in this paper compares a canard configuration and a conventional aft-tail configuration for a subsonic, medium-range transport aircraft. The choice of a commercial transport allows the use of an economic performance measure as a design figure of merit during trade studies. The design program contains an iterative optimization scheme which includes induced drag, parasite drag, trim drag, weight, variable flight paths, and mission parameters. This level of detail in the optimization scheme, when applied uniformly to a canard configuration and to a conventional aft-tail configuration, allows for a fair comparison for this class of aircraft. Two design parameters which are particularly sensitive for this class of aircraft are identified and studied. These parameters are the maximum lift coefficient $C_{L,\max}$ of the horizontal stabilizer and the main-landing-gear longitudinal position.

The requirement of achieving a large $C_{L,\max}$ is imposed on the horizontal stabilizer of a statically stable canard configuration for aircraft trim. This is particularly critical for transport aircraft since an efficient design must achieve a very high C_L during approach and landing. Even unstable canard configurations will require a much higher canard-surface $C_{L,\max}$ than that of current transport horizontal stabilizers. The required large $C_{L,\max}$ will dictate use of a high-lift system that must provide control-surface modulation as well as contribute to the overall aircraft lift. Such a high-lift control surface suitable for a commercial transport has neither been designed nor demonstrated.

The main-landing-gear position for a canard configuration will be forward of the wing-root leading edge. This requirement is dictated by the control-power requirement for nose-gear unstick during take-off. The main gear in this position will require a pod or a nacelle to house the stowed gear, creating a drag penalty. Further, since the landing loads will not be easily transferred to the wing spar structure, the fuselage in this area may need to be strengthened. This structural reinforcement will create a weight penalty. Other penalties may also exist and would require identification and assessment.

Given these design problems, it was difficult during the course of this study to find an economically feasible design for a canard configuration. If both the $C_{L,\max}$ limit on the control surface and the landing-gear placement problems are ignored, the canard configuration has approximately 2-percent better performance. This benefit is traceable to the criticality of achieving high lift during take-off and landing and is observable even though it is generally accepted that a canard configuration will have higher induced drag.

A special case of tandem-winged transports was studied, and this configuration was shown to be economically inferior to the canard configuration and to the conventional aft-tail configuration. It seems unlikely that the hypothetical benefits of manufacturing two "identical" lifting surfaces would be substantial enough to permit economically successful medium-range transports with tandem wings.

The ability to design medium-range transports with unstable static margins will apparently not benefit a canard configuration as much as previously thought because of compromises forced by configuration induced drag penalties. In fact, conventional configurations show more incremental economic benefits from unstable static margins than do canard configurations.

The results of this study tend to indicate that conventional aft-tail configurations are economically superior to canard configurations for this class of aircraft. Even when constraints are impractically reduced, the resulting canard configuration is only slightly better than a comparable conventional design. A possible alternative which could be used to solve these design problems while maintaining the benefits of both configurations would be a configuration with three lifting surfaces. Further research is needed to evaluate this transport configuration with a wing, a canard, and an aft-tail.

NASA Langley Research Center
Hampton, VA 23665
November 29, 1984

Appendix A

Approximation of Required Horizontal-Stabilizer $C_{L,\max}$ for a Statically Stable Canard Configuration

The required horizontal-stabilizer C_L of a trimmed, statically stable canard configuration may be approximated as follows. Figure A1 is a schematic of a generic

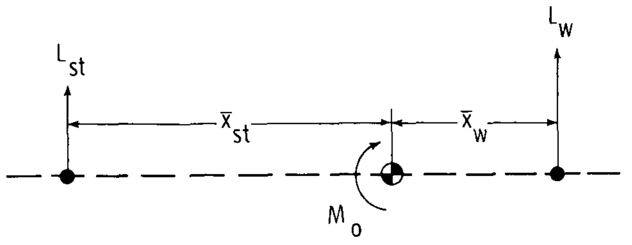

Figure A1. Schematic of trimmed canard configuration.

canard-configured transport. A simple trim equation which ignores drag terms is

$$\bar{x}_{st} L_{st} - \bar{x}_w L_w + M_o = 0 \qquad \text{(A1)}$$

where L_{st}, L_w, and M_o are normalized by dynamic pressure. Assume that $C_{m,o} = 0$; therefore, $M_o = 0$. Then, from equation (A1),

$$\bar{x}_{st} L_{st} - \bar{x}_w L_w = 0 \qquad \text{(A2)}$$

Dividing equation (A2) by S_w gives

$$\bar{x}_{st} \frac{L_{st}}{S_w} - \bar{x}_w \frac{L_w}{S_w} = 0$$

$$\bar{x}_{st} \frac{S_{st}}{S_w} \frac{L_{st}}{S_{st}} - \bar{x}_w \frac{L_w}{S_w} = 0 \qquad \text{(A3)}$$

Note that

$$C_L = \frac{L}{S}$$

where L is lift normalized by dynamic pressure; thus, equation (A3) becomes

$$\bar{x}_{st} \frac{S_{st}}{S_w} C_{L,st} - \bar{x}_w C_{L,w} = 0$$

or

$$\frac{\bar{x}_{st} S_{st}}{\bar{x}_w S_w} = \frac{C_{L,w}}{C_{L,st}} \qquad \text{(A4)}$$

From equation (A2), static stability for a trimmed canard configuration (fig. A1) can be expressed as

$$\bar{x}_w \, \Delta L_w > \bar{x}_{st} \, \Delta L_{st} \qquad \text{(A5)}$$

Since

$$\Delta L = C_{L_\alpha} S \, \Delta\alpha$$

substitution into equation (A5) gives

$$C_{L_{\alpha,w}} S_w \bar{x}_w > C_{L_{\alpha,st}} S_{st} \bar{x}_{st} \qquad \text{(A6)}$$

or

$$\frac{C_{L_{\alpha,w}} S_w \bar{x}_w}{C_{L_{\alpha,st}} S_{st} \bar{x}_{st}} > 1 \qquad \text{(A7)}$$

Substituting the result of equation (A4) yields

$$\frac{C_{L_{\alpha,w}}}{C_{L_{\alpha,st}}} \frac{C_{L,st}}{C_{L,w}} > 1$$

or

$$\frac{C_{L,st}}{C_{L_{\alpha,st}}} > \frac{C_{L,w}}{C_{L_{\alpha,w}}}$$

Typically, $C_{m,o}$ is negative (pitch-down condition). By examining figure A1, we see that this condition requires even more $C_{L,st}$ for trim. If we assume $C_{L_{\alpha,st}} \approx C_{L_{\alpha,w}}$, then for a statically stable canard transport configuration,

$$C_{L,st} > C_{L,w} \qquad \text{(A8)}$$

for all trimmed-flight regimes. Therefore,

$$C_{L,st,\max} > C_{L,w,\max}$$

Appendix B

Qualitative Examination of Take-Off Control-Power Requirement

Figure B1 is a schematic of the physics of the take-off control-power requirement for a conventional configuration. From an examination of the moments about the c.g., it is seen that to rotate the aircraft, the horizontal stabilizer must provide a downward load to overcome the pitch-down moments generated by wing-body zero-lift moment ($M_o < 0$) plus the reaction at the landing gear. Note that some pitch-up moment is already being provided by wing lift and the thrust vector.

A schematic for a canard configuration is shown in figure B2. Since the main landing gear must be in the same position relative to the aircraft c.g. to maintain nosewheel traction, this contribution to the moment about the c.g. remains about the same as for the conventional configuration. Also, the thrust contribution and the wing-body zero-lift pitching-moment contribution will be about the same as for a conventional configuration. However, since the wing is aft of the c.g., the pitching-moment contribution due to wing lift will be downward. Therefore, the canard surface will have to provide enough lift to balance the pitch-down contributions of wing-body zero-lift moment, reaction at the landing gear, and wing lift, less the pitch-up contribution of engine thrust. The lift demands placed on the canard surface far exceed the downward load demands placed on a conventional configuration's horizontal stabilizer. This is why the take-off control-power requirement is critical for canard configurations.

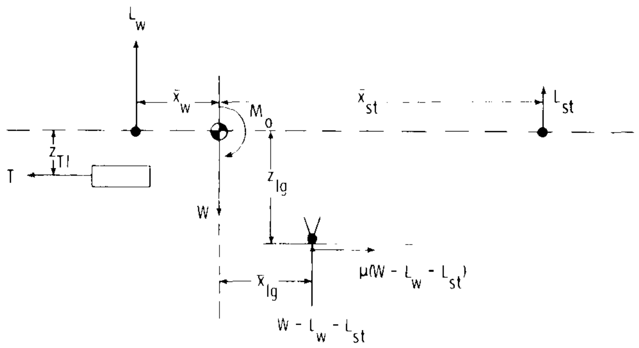

Figure B1. Schematic of conventional configuration during take-off roll.

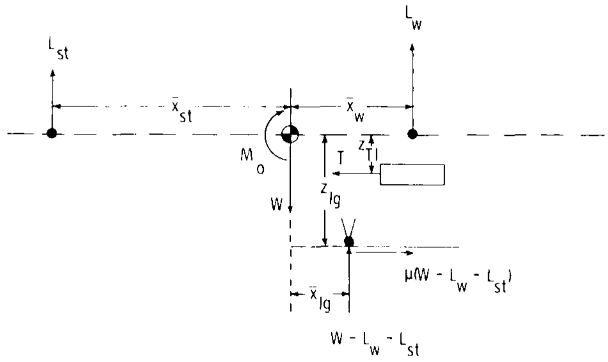

Figure B2. Schematic of canard configuration during take-off roll.

References

1. Burns, B. R. A.: Were the Wrights Right? *Air Int.*, vol. 25, no. 6, Dec. 1983, pp. 285–292, 308–309.
2. Sliwa, Steven M.; and Arbuckle, P. Douglas: *OPDOT: A Computer Program for the Optimum Preliminary Design of a Transport Airplane.* NASA TM-81857, 1980.
3. Sliwa, Steven M.: *Use of Constrained Optimization in the Conceptual Design of a Medium-Range Subsonic Transport.* NASA TP-1762, 1980.
4. Sliwa, Steven M.: Sensitivity of the Optimal Preliminary Design of a Transport to Operational Constraints and Performance Index. AIAA-80-1895, Aug. 1980.
5. Sliwa, Steven M.: *Economic Evaluation of Flying-Qualities Design Criteria for a Transport Configured With Relaxed Static Stability.* NASA TP-1760, 1980.
6. Sliwa, Steven M.: Impact of Longitudinal Flying Qualities Upon the Design of a Transport With Active Controls. *A Collection of Technical Papers—AIAA Atmospheric Flight Mechanics Conference*, Aug. 1980, pp. 133–141. (Available as AIAA-80-1570.)
7. Hall, Charles F.; and Boyd, John W.: *Effects of Canards on Airplane Performance and Stability.* NACA RM A58D24, 1958.
8. Gloss, Blair B.; Ray, Edward J.; and Washburn, Karen E.: *Effect of Canard Vertical Location, Size, and Deflection on Canard-Wing Interference at Subsonic Speeds.* NASA TM-78790, 1978.
9. McLaughlin, Milton D.: *Calculations, and Comparison With an Ideal Minimum, of Trimmed Drag for Conventional and Canard Configurations Having Various Levels of Static Stability.* NASA TN D-8391, 1977.
10. McGeer, Tad; and Kroo, Ilan: A Fundamental Comparison of Canard and Conventional Configurations. *J. Aircr.*, vol. 20, no. 11, Nov. 1983, pp. 983–992.
11. Kroo, I. M.; and McGeer, T.: Optimization of Canard Configurations—An Integrated Approach and Practical Drag Estimation Method. *ICAS Proceedings—1982*, B. Laschka and R. Staufenbiel, eds., 1982, pp. 1459–1469. (Available as ICAS-82-6.8.1.)
12. Butler, G. F.: An Analytical Study of the Induced Drag of Canard-Wing-Tail Aircraft Configurations With Various Levels of Static Stability. *Aeronaut. J.*, vol. 87, no. 868, Oct. 1983, pp. 293–300.
13. Laitone, E. V.: Prandtl's Biplane Theory Applied to Canard and Tandem Aircraft. *J. Aircr.*, vol. 17, no. 4, Apr. 1980, pp. 233–237.
14. Laitone, E. V.: Positive Tail Loads for Minimum Induced Drag of Subsonic Aircraft. *J. Aircr.*, vol. 15, no. 12, Dec. 1978, pp. 837–842.
15. Feistel, T. W.; Corsiglia, V. R.; and Levin D. B.: Wind-Tunnel Measurements of Wing-Canard Interference and a Comparison With Various Theories. *SAE 1981 Transactions*, Section 2, Volume 90, 1982, pp. 2026–2039. (Available as SAE Paper 810575.)
16. Yip, Long P.; and Coy, Paul F.: Wind-Tunnel Investigation of a Full-Scale Canard-Configured General Aviation Aircraft. *Proceedings of the 13th Congress of the International Council of the Aeronautical Sciences and AIAA Aircraft Systems and Technology Conference, Volume 2*, B. Laschka and R. Staufenbiel, eds., 1982, pp. 1470–1488. (Available as ICAS-82-6.8.2.)
17. Rutan, Burt: Development of a Small High-Aspect-Ratio Canard Aircraft. *1976 Report to the Aerospace Profession*, Tech. Rev., vol. 13, no. 2, Soc. Exp. Test Pilots, 1976, pp. 93–101.
18. Chambers, Joseph R.; Yip, Long P.; and Moul, Thomas M.: *Wind-Tunnel Investigation of an Advanced General Aviation Canard Configuration.* NASA TM-85760, 1984.
19. Selberg, B. P.: Aerodynamic Investigation of Closely Coupled Lifting Surfaces With Positive and Negative Stagger for General Aviation Applications. AIAA-83-0057, Jan. 1983.
20. Keith, Michael W.; and Selberg, Bruce P.: Aerodynamic Optimization, Comparison, and Trim Design of Canard and Conventional High Performance General Aviation Configurations. AIAA-83-0058, Jan. 1983.
21. Keith, Michael W.; and Selberg, Bruce P.: Aerodynamic Canard/Wing Parametric Analysis for General Aviation Applications. AIAA-84-0560, Jan. 1984.
22. Srivatsan, R.; and Roskam, Jan: Unconventional Commuter Configurations: A Design Investigation. SAE Tech. Paper Ser. 830710, Apr. 1983.
23. Olsson, D. M.: A Sequential Simplex Program for Solving Minimization Problems. *J. Qual. Technol.*, vol. 6, no. 1, Jan. 1974, pp. 53–57.
24. Olsson, Donald M.; and Nelson, Lloyd S.: The Nelder-Mead Simplex Procedure for Function Minimization. *Technometrics*, vol. 17, no. 1, Feb. 1975, pp. 45–51.
25. Nicolai, Leland M.: *Fundamentals of Aircraft Design.* School of Eng., Univ. of Dayton, Dayton, Ohio, c.1975.
26. Oman, B. H.: *Vehicle Design Evaluation Program.* NASA CR-145070, 1977.
27. Anderson, R. D.; Flora, C. C.; Nelson, R. M.; Raymond, E. T.; and Vincent, J. H.: *Development of Weight and Cost Estimates for Lifting Surfaces With Active Controls.* NASA CR-144937, 1976.
28. Kyser, Albert C.: *An Elementary Analysis of the Effect of Sweep, Mach Number, and Lift Coefficient on Wing-Structure Weight.* NASA TM-74072, 1977.
29. Aggarwal, R.; et al.: *An Analysis of Fuel Conserving Operational Procedures and Design Modifications for Bomber/Transport Aircraft—Volume II.* AFFDL-TR-78-96, Vol. II, U.S. Air Force, July 1978. (Available from DTIC as AD A062 609.)
30. Perkins, Courtland D.; and Hage, Robert E.: *Airplane Performance Stability and Control.* John Wiley & Sons, Inc., c.1949.
31. Hoerner, Sighard F.: *Fluid-Dynamic Drag.* Hoerner Fluid Dynamics (Brick Town, N.J.), c.1965.
32. Loftin, Laurence K., Jr.: *Subsonic Aircraft: Evolution and the Matching of Size to Performance.* NASA RP-1060, 1980.
33. *USAF Stability and Control Datcom.* Contracts AF33 (616)-6460 and F33615-76-C-3061, McDonnell Douglas Corp., Oct. 1960. (Rev. Apr. 1978.)
34. Roskam, Jan: *Methods for Estimating Stability and Control Derivatives of Conventional Subsonic Airplanes.*

Pub. by the author (Dep. Aerosp. Eng., Univ. of Kansas, Lawrence, Kansas), c.1973.

35. Harris, Charles D.: *Aerodynamic Characteristics of a 14-Percent-Thick NASA Supercritical Airfoil Designed for a Normal-Force Coefficient of 0.7.* NASA TM X-72712, 1975.
36. Bartlett, Dennis W.: *Wind-Tunnel Investigation of Several High Aspect-Ratio Supercritical Wing Configurations on a Wide-Body-Type Fuselage.* NASA TM X-71996, 1977.
37. Heffley, R. K.; et al.: *Aircraft Handling Qualities Data.* NASA CR-2144, 1972.
38. Seckel, Edward: *Stability and Control of Airplanes and Helicopters.* Academic Press, Inc., c.1964.
39. McRuer, Duane; Ashkenas, Irving; and Graham, Dunstan: *Aircraft Dynamics and Automatic Control.* Princeton Univ. Press, 1973.
40. American Airlines: *A New Method for Estimating Current and Future Transport Aircraft Operating Economics.* NASA CR-145190 (Rev.), 1978.
41. Maddalon, Dal V.: *Estimating Airline Operating Costs.* NASA TM-78694, 1978.
42. Stoessel, Robert F.: *A Proposed Standard Method for Estimating Airline Indirect Operating Expense.* Rep. No. LW70-500R, Lockheed-Georgia Co., May 1970.
43. *Assessment of the Application of Advanced Technologies to Subsonic CTOL Transport Aircraft.* NASA CR-112242, 1973.
44. Boeing Commercial Airplane Co.: *Integrated Application of Active Controls (IAAC) Technology to an Advanced Subsonic Transport Project—Initial ACT Configuration Design Study, Final Report.* NASA CR-159249, 1980.

TABLE I. DEFINING PARAMETERS FOR OPDOT

(a) Independent design variables

Independent design variable	Lower limit	Upper limit
Wing area, S_w, ft^2	1000	4000
Wing aspect ratio, AR_w	3	15
Horizontal-stabilizer area, S_{st}, ft^2	200	3000
Horizontal-stabilizer aspect ratio, AR_{st}	2	15
Aftmost c.g., x'_{cg}, percent MAC	−500	100
Installed thrust, T, lb	10 000	130 000
Fuselage length, l_f, ft	100	220
Horizontal-stabilizer longitudinal position, x_{st}, percent l_f:		
Canard configuration	12.5	47.5
Conventional configuration	70.5	97.5
Main-landing-gear longitudinal position, x_{lg}, percent MAC:		
Canard configuration	−250	0
Conventional configuration	0	200

(b) Available constraint functions

Available constraint function	Baseline function limit
Thrust for cruise-climb	$T_{av}/T_{req} \geq 1$
Second-segment climb gradient	$T_{av}/T_{req} \geq 1$
Missed-approach climb gradient	$T_{av}/T_{req} \geq 1$
Landing field length, ft	≤ 8000
Take-off field length, ft	≤ 8000
Nosewheel steering traction	$x'_{cg} \leq x_{lg} - NG$
Passenger volume	$V_{p,req}/V_{p,av} \leq 1$
Cruise altitude, ft	$30\,000 \leq h_{cr} \leq 46\,000$
Cruise wing lift coefficient	≤ 0.7
Static margin, SM, (cruise and approach), percent MAC	≤ 10
Horizontal-stabilizer longitudinal position, ft aft of nose	≥ 20
Horizontal-stabilizer lift coefficient in approach	$-0.80 \leq C_{L,st} \leq 3.15$
Nose-gear unstick	$L_{st,av}/L_{st,req} \geq 1$

TABLE II. KEY DESIGN CONSTANTS USED FOR DESIGN OPTIMIZATION

[Supercritical airfoils and curved windshield assumed]

Mission:	
Cruise Mach number	0.80
Divergence Mach number	0.84
Design range, n.mi.	3000
Number of seats	200
Cargo, lb	7500
Maximum lift coefficient	3.15
Geometry:	
Wing longitudinal position, percent l_f:	
Conventional configuration	50
Canard configuration	72
Wing sweep angle, deg:	
Conventional configuration	25
Canard configuration	20
Horizontal-stabilizer sweep angle, deg:	
Conventional configuration	35
Canard configuration	22
Height of horizontal stabilizer above fuselage centerline, ft:	
Conventional configuration	7.0
Canard configuration	−2.5
Wing thickness ratio	0.14
Wing taper ratio	0.38
Wing incidence angle, deg	2
Wing geometric twist, deg	5
Horizontal-stabilizer thickness ratio	0.10
Horizontal-stabilizer taper ratio	0.4
Vertical-stabilizer sweep, deg	35
Ratio of rudder area to vertical-stabilizer area	0.30
Ratio of elevator chord to horizontal-stabilizer chord	0.25
Ratio of flap span to wing span	0.6
Maximum flap deflection, deg	45
Fuselage diameter, ft	16.67
Distance of thrust vector below c.g., ft	6
Number of engines	2
Wing dihedral, deg	5
Economics:	
Fuel cost, dollars per gallon	1.00
Load factor	0.55
Utilization rate, hours per year	3200
Depreciation period, years	14
Residual value, percent	12
Tax rate	0.48
Year of study	1982
Assumed annual inflation rate	0.07
Number of prototype aircraft	2
Aircraft fleet size	250
Initial production rate, per month	0.5
Full production rate, per month	5
Engineering rate (1974), dollars per hour	19.55
Tooling rate (1974), dollars per hour	14.00

TABLE II. Concluded

Labor rate (1974), dollars per hour	10.90
Engines for test aircraft	3
Ratio of manufacturer's airframe weight to take-off weight	0.75
Miscellaneous:	
Maximum dynamic pressure, psf	245.6
Pressurized volume, ft^3	6290
Number of pilots	3
Number of attendants	8
Air conditioning flow rate, lb/min	441
Autopilot channels	5
Generator capacity, kV-A	750
Maintenance complexity factor	1.6
Hydraulics volume flow rate, gal/min	79
Number of inertial platform systems	1
Ratio of auxiliary-power-unit-on time to engine-on time	0.1
Ratio of first class to economy seating	0.15
Maximum speed, knots	483
Airfoil design lift coefficient	0.5
Baseline engine	TF39-GE-1
Elevator servo time constant, sec	0.1

TABLE III. BASELINE CONFIGURATION VARIABLES

Variable	Canard configuration	Conventional configuration	Tandem-wing configuration
Wing area, ft^2	1748.2	2015.6	950.1
Wing aspect ratio	8.76	11.22	13.00
Horizontal-stabilizer area, ft^2	769.6	682.0	950.1
Horizontal-stabilizer aspect ratio	7.92	3.79	13.00
Aftmost center of gravity, percent MAC	−182	33	−341
Installed thrust, lb	66445.	68892.	73118.
Fuselage length, ft	160.0	164.0	166.3
Horizontal-stabilizer longitudinal position, percent l_f	19.03	97.36	28.89
Main-landing-gear longitudinal position, percent MAC	−114	65*	−233

*A design constant for this configuration.

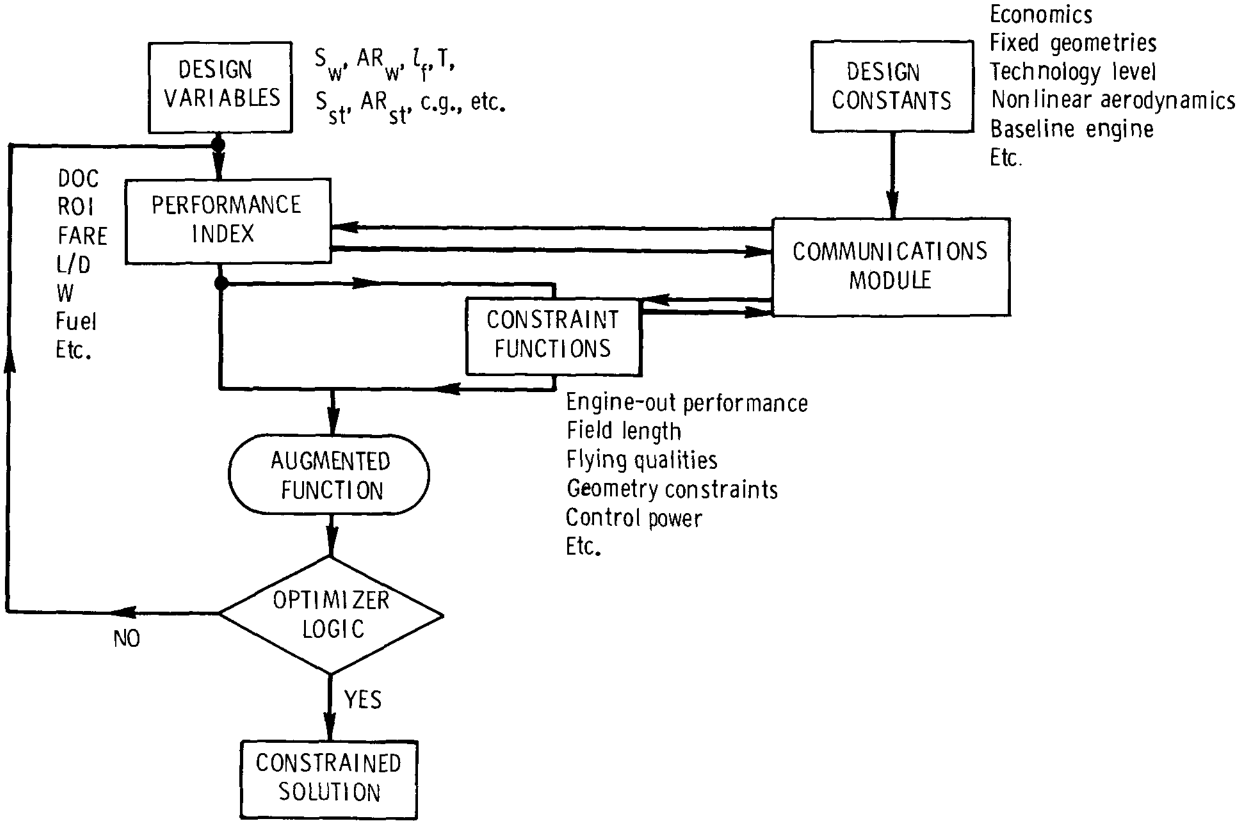

Figure 1. General optimization scheme for OPDOT.

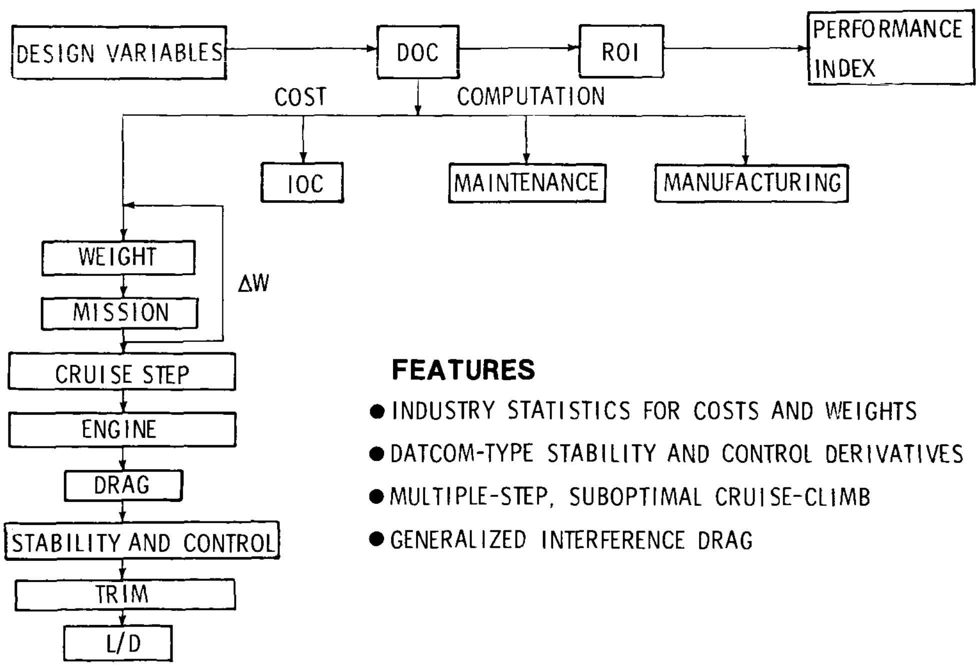

Figure 2. Performance-index evaluation routines for OPDOT.

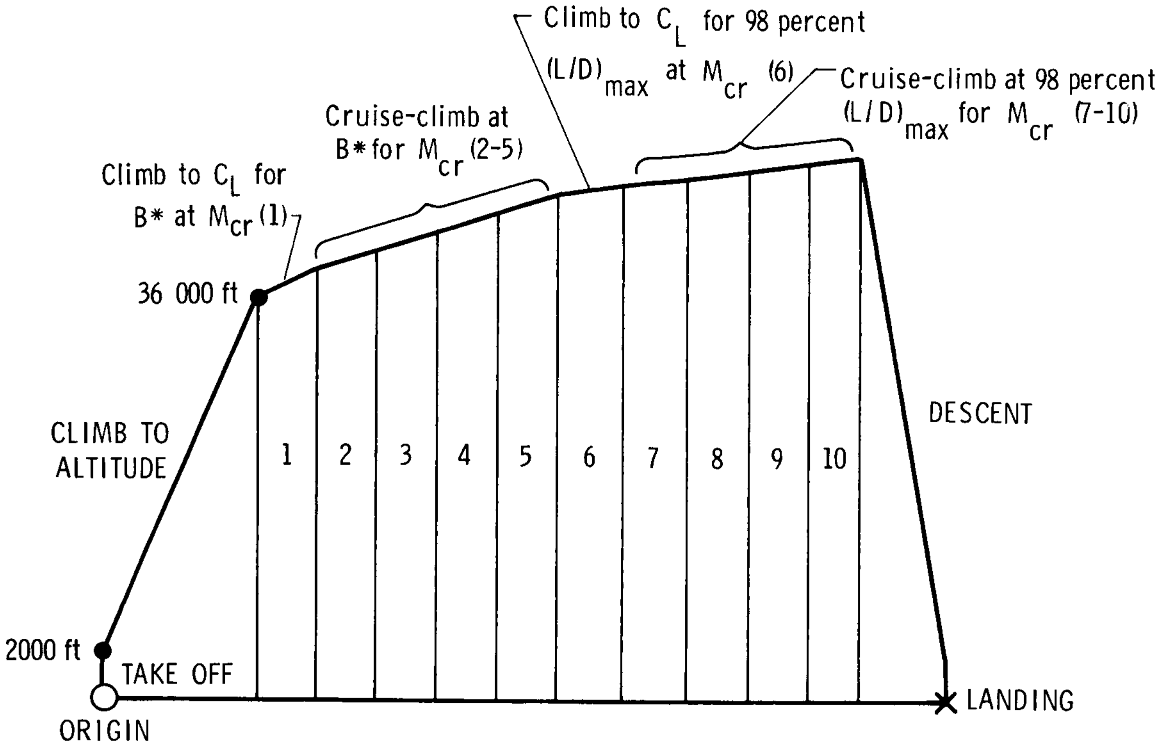

Figure 3. Mission profile from OPDOT.

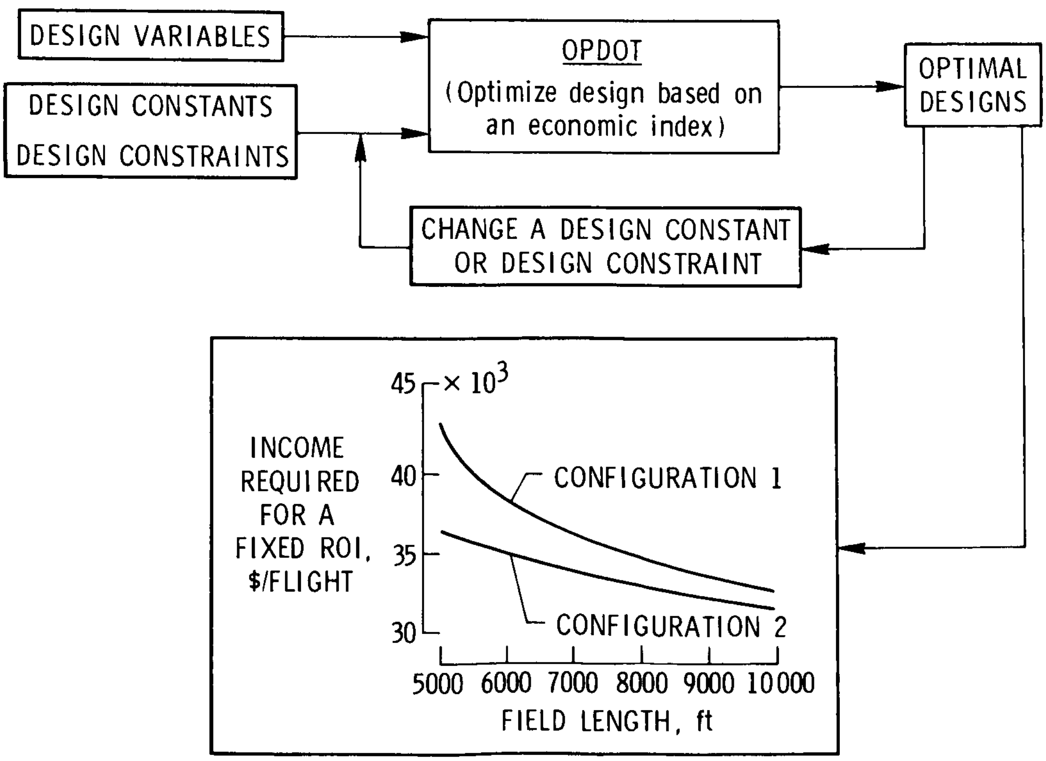

Figure 4. Methodology for conducting sensitivity studies with OPDOT.

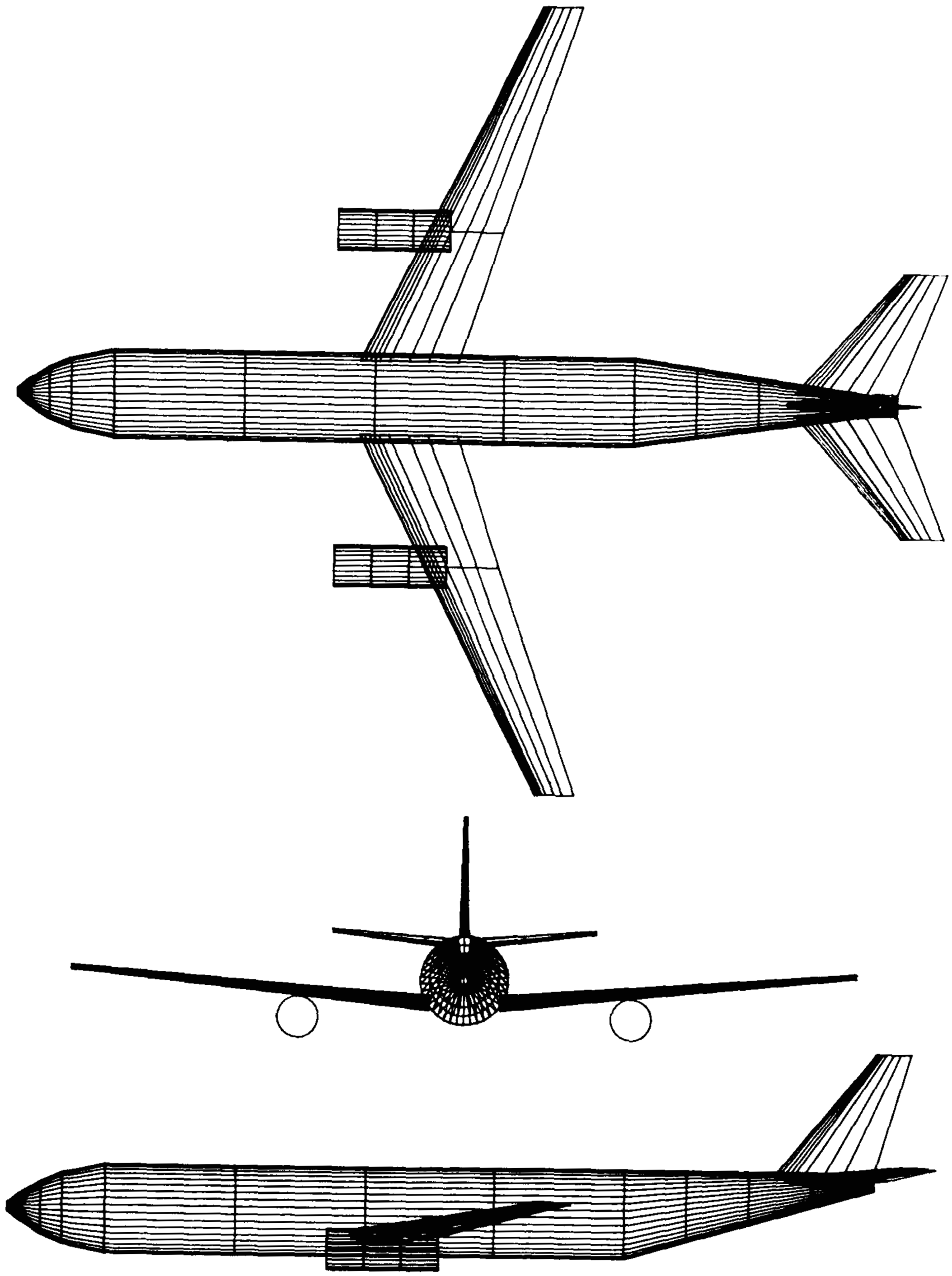

Figure 5. Three-view depiction of baseline conventional configuration.

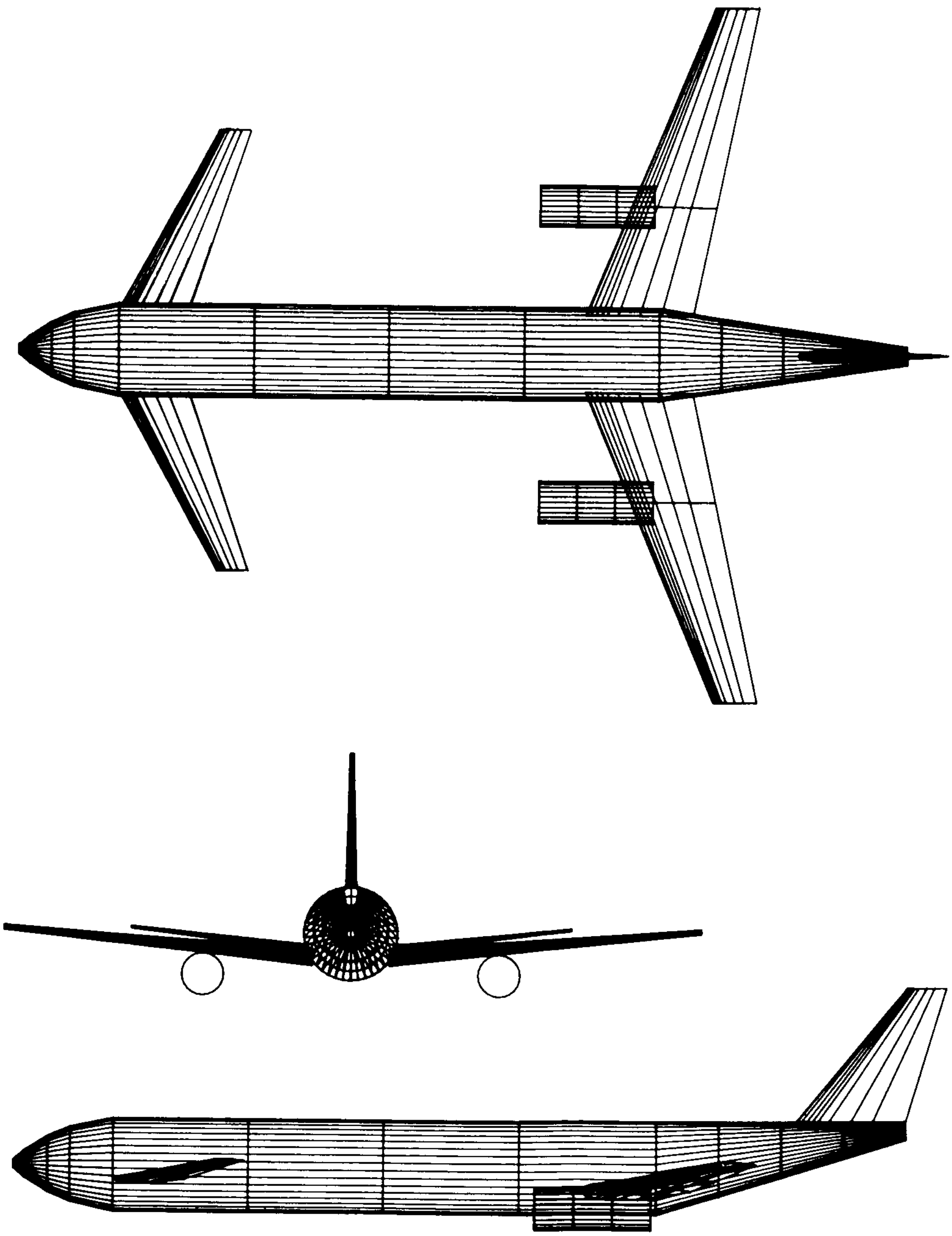

Figure 6. Three-view depiction of baseline canard configuration.

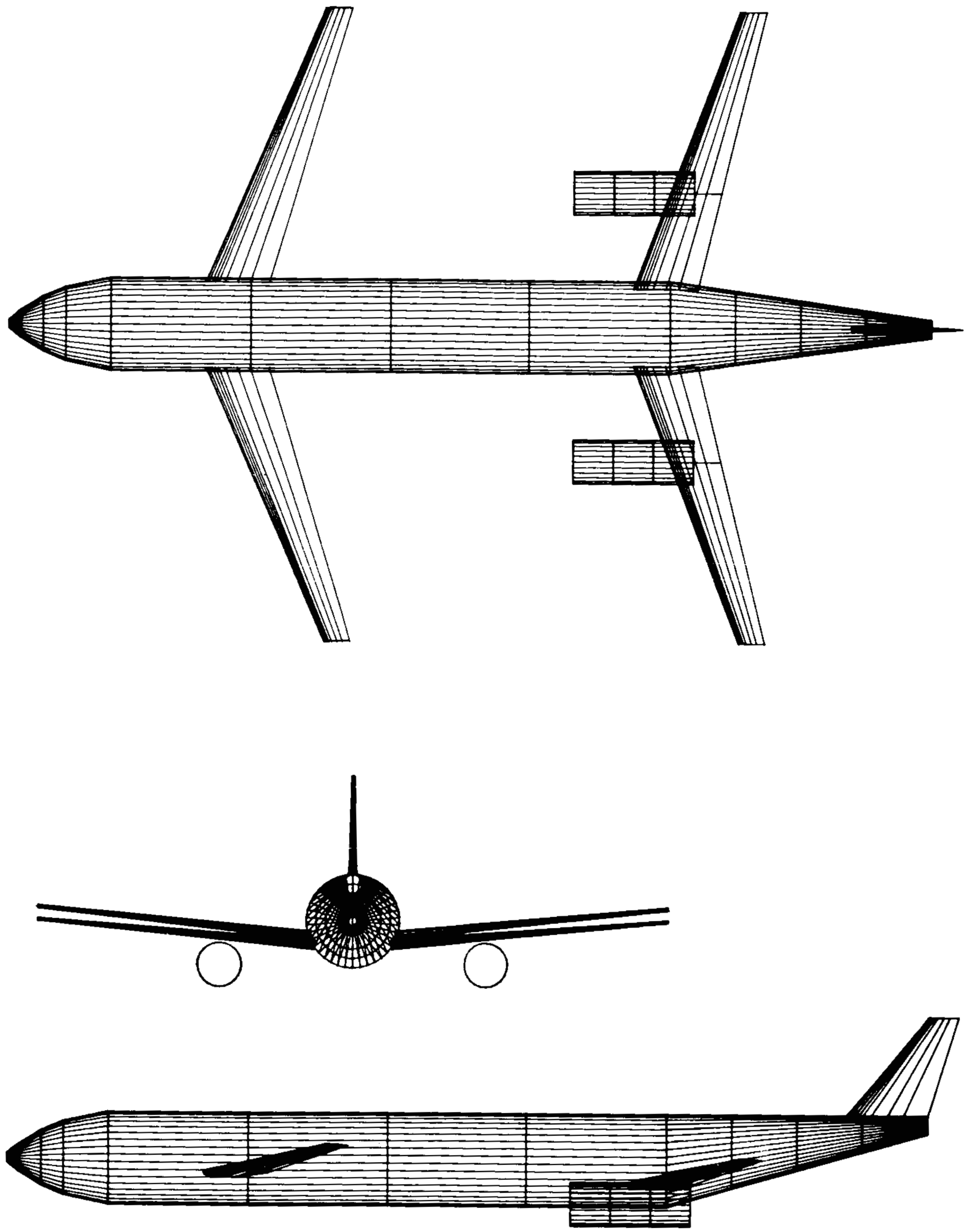

Figure 7. Three-view depiction of baseline tandem-wing configuration.

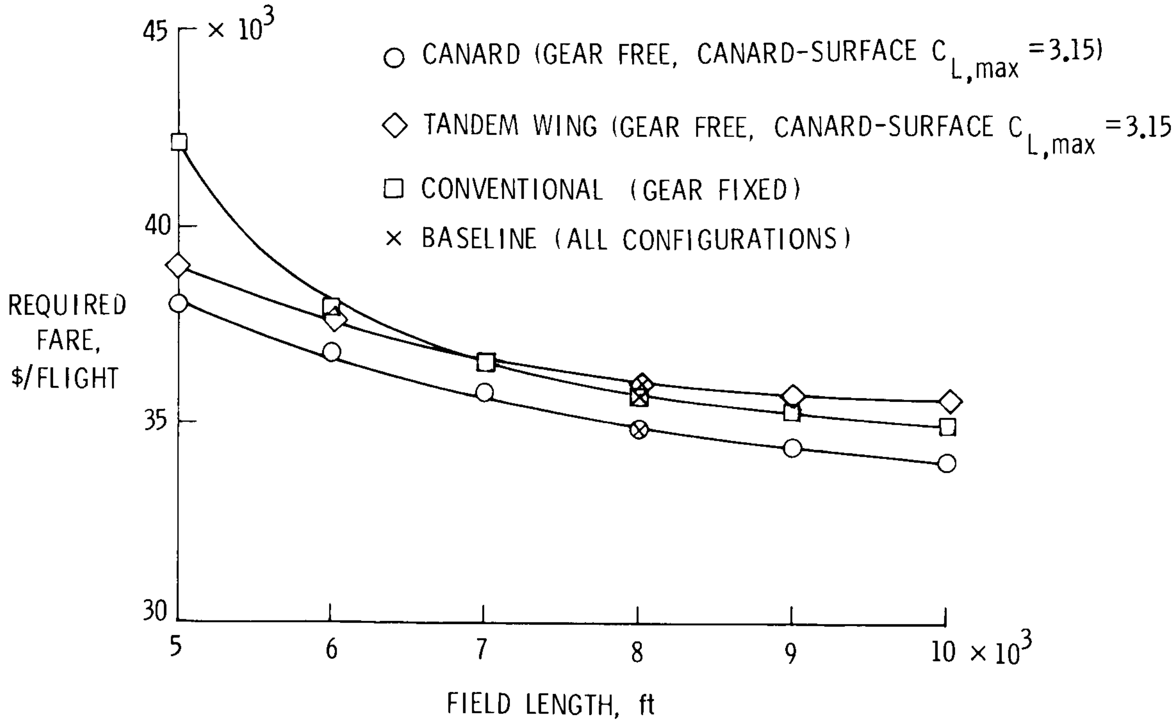

Figure 8. Effect of take-off–landing field length on required FARE. Static margin of 10 percent.

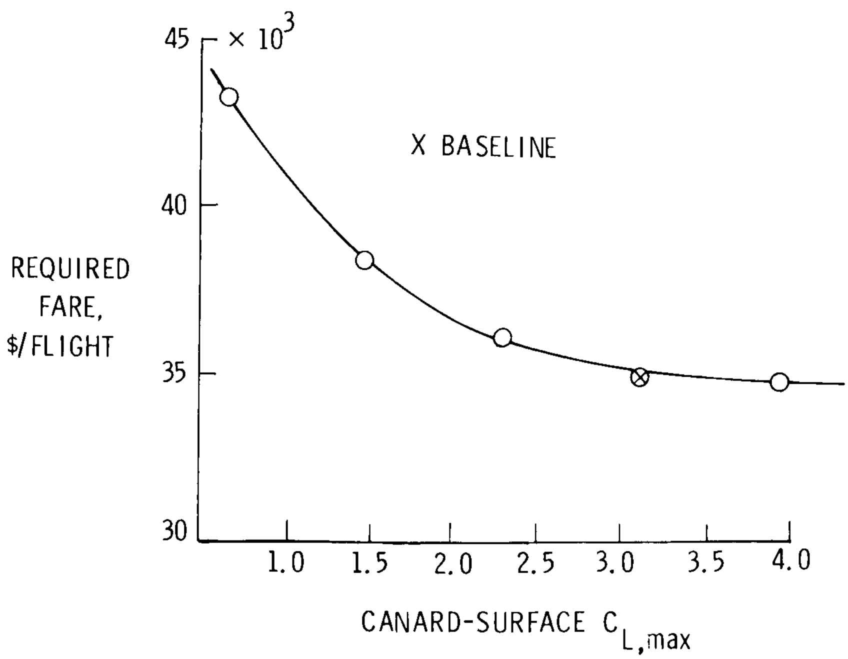

Figure 9. Effect of canard-surface $C_{L,\max}$ on required FARE. Static margin of 10 percent.

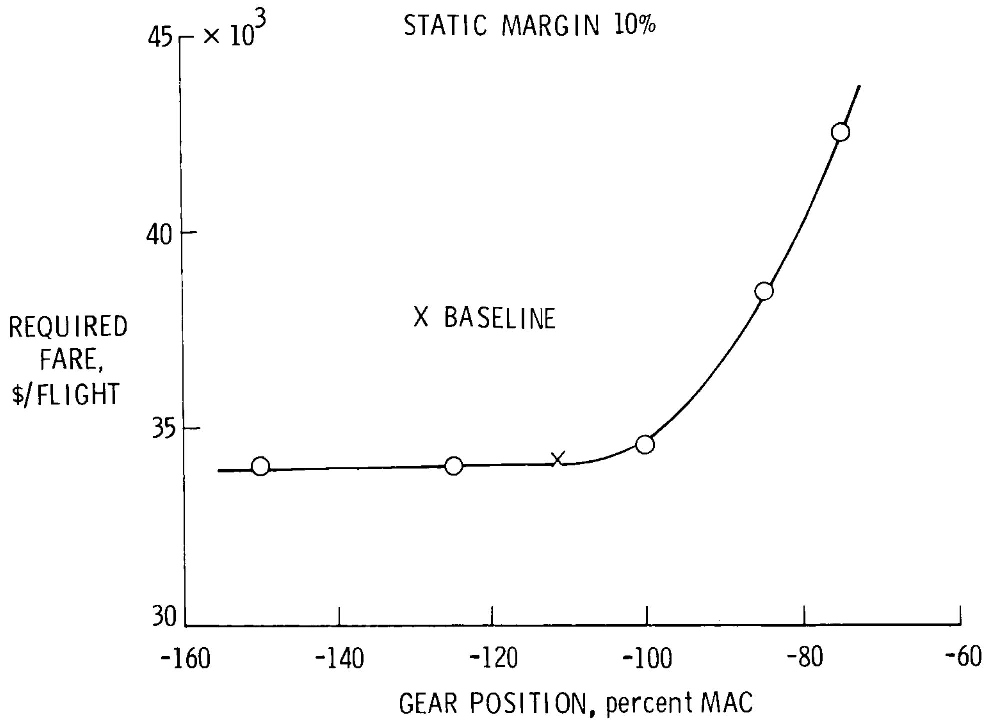

Figure 10. Effect on required FARE of main-landing-gear position for canard configuration. Static margin of 10 percent.

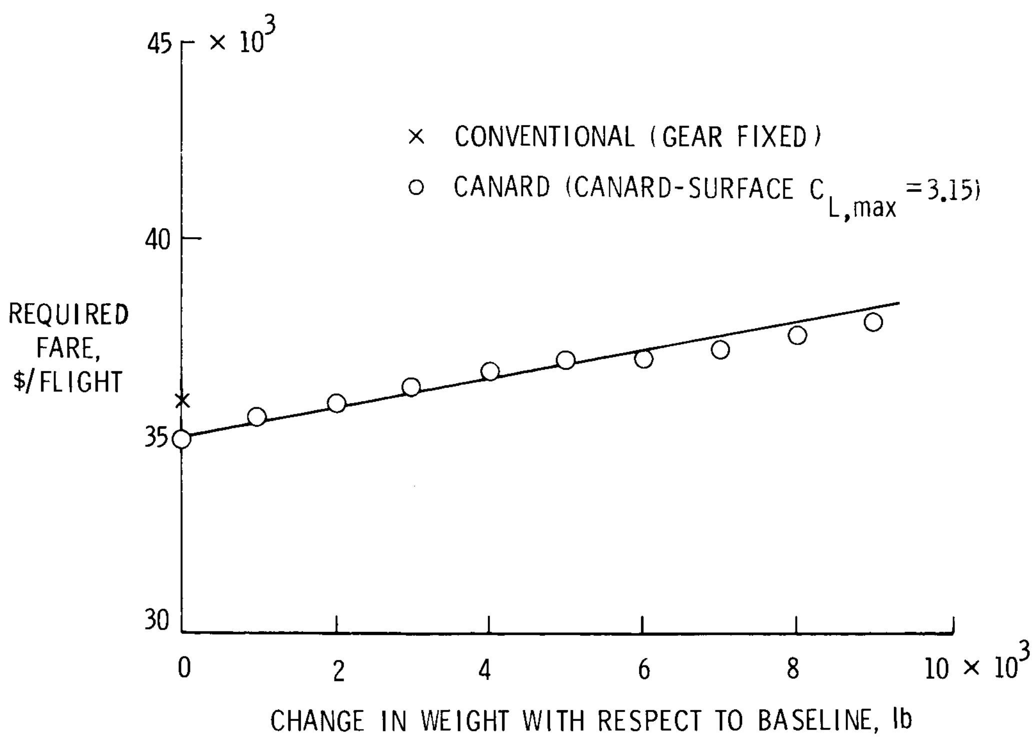

Figure 11. Effect of aircraft weight increase on required FARE for canard configuration. Static margin of 10 percent.

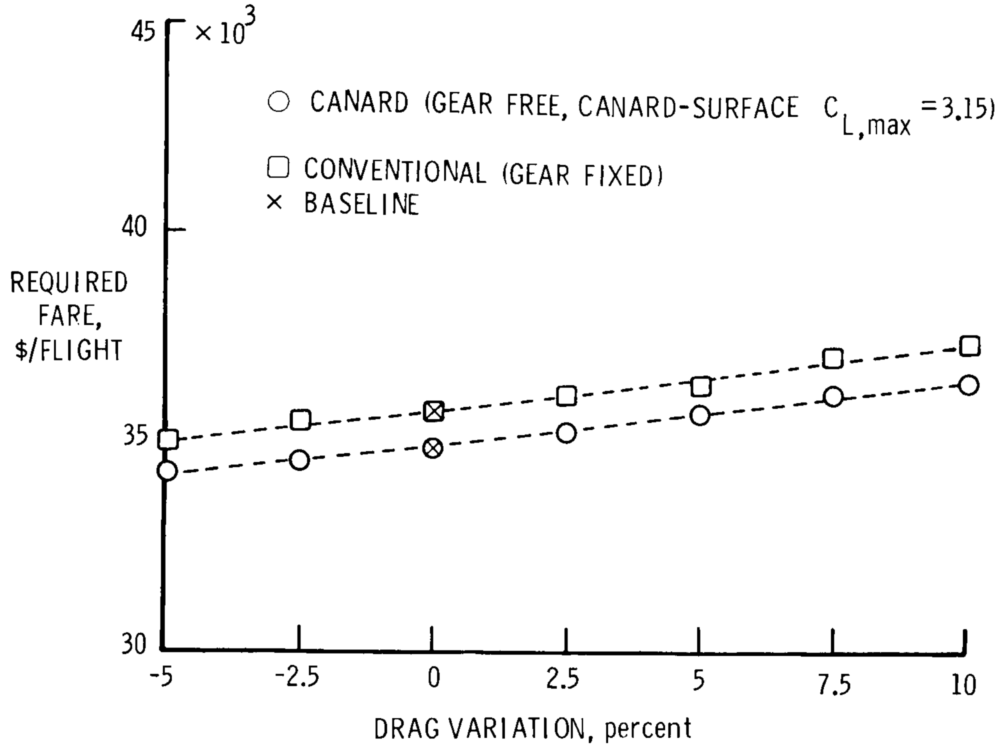

Figure 12. Effect of aircraft drag on required FARE. Static margin of 10 percent.

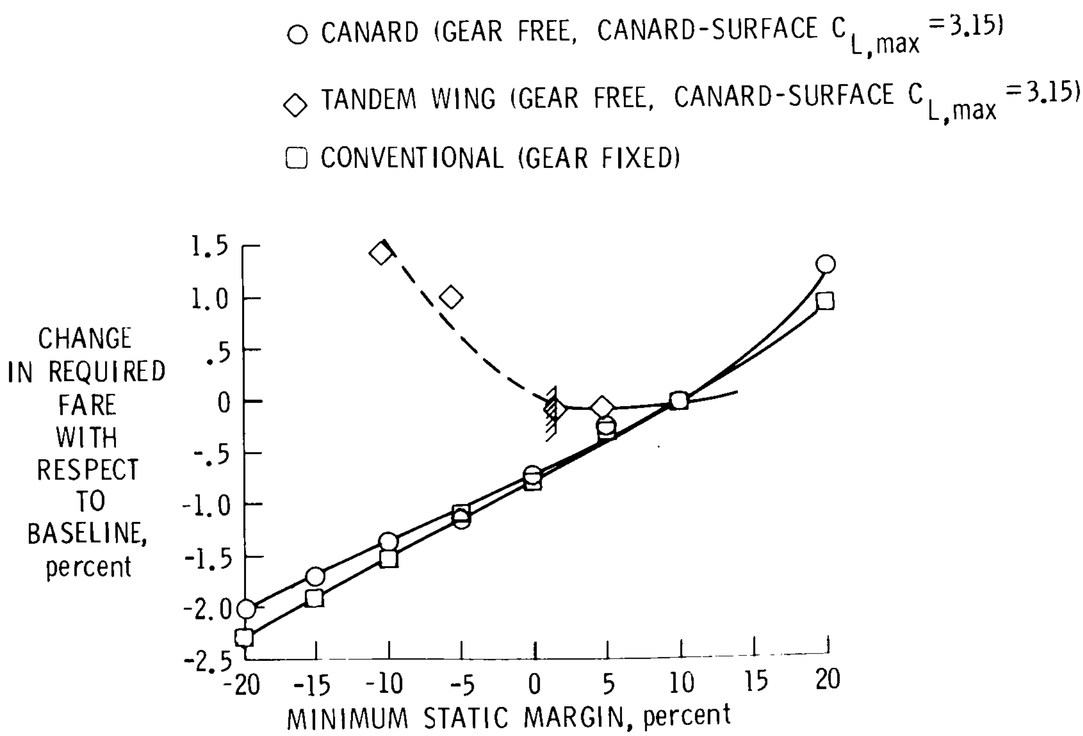

Figure 13. Effect of minimum static margin on percent change in required FARE.

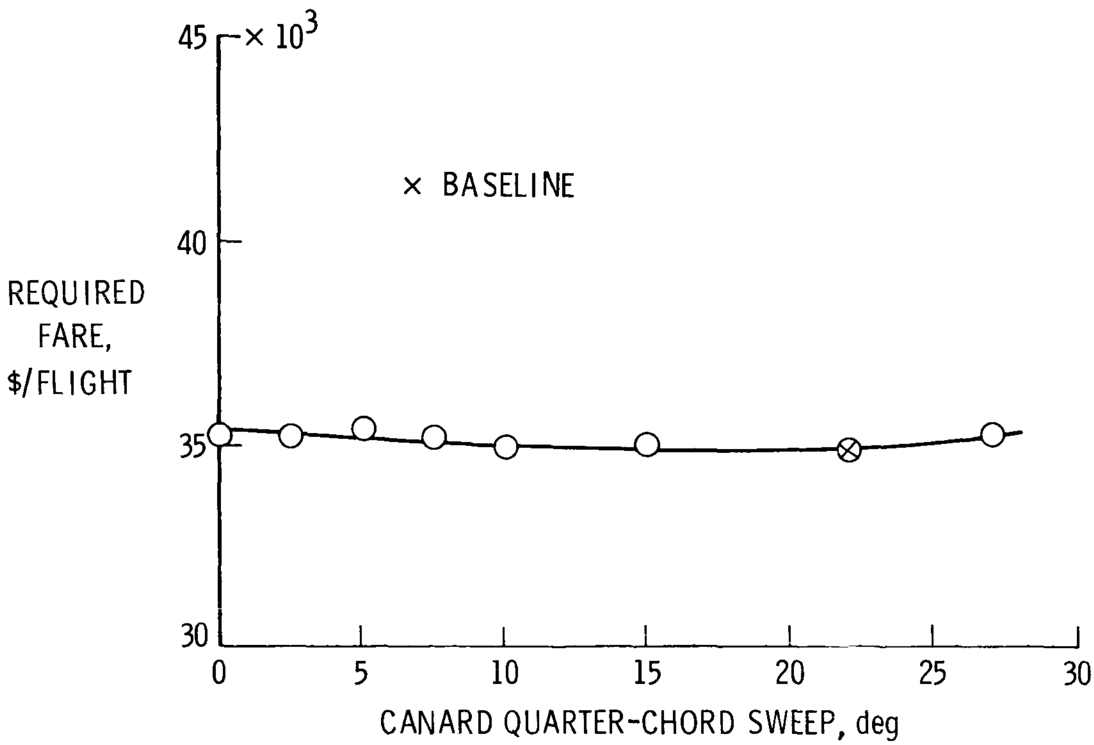

Figure 14. Effect of canard-surface sweep angle on required FARE. Static margin of 10 percent.

1. Report No.	2. Government Accession No.	3. Recipient's Catalog No.
NASA TP-2400		

4. Title and Subtitle Parametric Study of a Canard-Configured Transport Using Conceptual Design Optimization	5. Report Date March 1985
	6. Performing Organization Code 505-34-03-05
7. Author(s) P. Douglas Arbuckle and Steven M. Sliwa	8. Performing Organization Report No. L-15856
9. Performing Organization Name and Address NASA Langley Research Center Hampton, VA 23665	10. Work Unit No.
	11. Contract or Grant No.
12. Sponsoring Agency Name and Address National Aeronautics and Space Administration Washington, DC 20546	13. Type of Report and Period Covered Technical Paper
	14. Sponsoring Agency Code

15. Supplementary Notes

16. Abstract

Constrained-parameter optimization is used to perform optimal conceptual design of both canard and conventional configurations of a medium-range transport. A number of design constants and design constraints are systematically varied to compare the sensitivities of canard and conventional configurations to a variety of technology assumptions. Main-landing-gear location and canard surface high-lift performance are identified as critical design parameters for a statically stable, subsonic, canard-configured transport.

17. Key Words (Suggested by Authors(s))	18. Distribution Statement
Conceptual design Constrained optimization Sensitivity to design parameters Canard configuration Tandem-wing configuration Economic evaluation	Unclassified · Unlimited Subject Categories 05, 08

19. Security Classif.(of this report)	20. Security Classif.(of this page)	21. No. of Pages	22. Price
Unclassified	Unclassified	26	A03

For sale by the National Technical Information Service, Springfield, Virginia 22161

NASA-Langley, 1985